AD-A096 695 NAVAL RESEARCH LAB WASHINGTON DC F/G 4/1
A COHERENT NONLINEAR THEORY OF AURORAL KILOMETRIC RADIATION. II--ETC(U)
MAR 81 C L GRABBE, P J PALMADESSO
UNCLASSIFIED NRL-MR-4440 NL

END
4-81

SECURITY CLASSIFICATION OF THIS PAGE *(When Data Entered)*

(9) **REPORT DOCUMENTATION PAGE**

READ INSTRUCTIONS BEFORE COMPLETING FORM

1. REPORT NUMBER	2. GOVT ACCESSION NO.	3. RECIPIENT'S CATALOG NUMBER
NRL Memorandum Report 4440	AD-A096 895	

4. TITLE *(and Subtitle)*

(6) A COHERENT NONLINEAR THEORY OF AURORAL KILOMETRIC RADIATION: II. DYNAMIC INTERACTIONS

5. TYPE OF REPORT & PERIOD COVERED
Interim report on a continuing NRL problem.

6. PERFORMING ORG. REPORT NUMBER

7. AUTHOR(s)

(10) Crockett L. Grabbe* Peter J. Palmadesso

8. CONTRACT OR GRANT NUMBER(s)
(16) RR033 02

9. PERFORMING ORGANIZATION NAME AND ADDRESS
Naval Research Laboratory
Washington, D.C. 20375

10. PROGRAM ELEMENT, PROJECT, TASK AREA & WORK UNIT NUMBERS
(14) 61153N; RR0330244; 47-0884-0-1.

11. CONTROLLING OFFICE NAME AND ADDRESS
Office of Naval Research
Arlington, VA. 22217
(11) 27 Mar 81

12. REPORT DATE
March 27, 1981

13. NUMBER OF PAGES
24
(12) 25

14. MONITORING AGENCY NAME & ADDRESS *(if different from Controlling Office)*
(14) NRL-MR-4440

15. SECURITY CLASS. *(of this report)*
UNCLASSIFIED

15a. DECLASSIFICATION/DOWNGRADING SCHEDULE

16. DISTRIBUTION STATEMENT *(of this Report)*

Approved for public release; distribution unlimited.

17. DISTRIBUTION STATEMENT *(of the abstract entered in Block 20, if different from Report)*

18. SUPPLEMENTARY NOTES

This research was sponsored by the Office of Naval Research under project No. RR0330244.
*Science Applications, Inc., McLean, VA. 22102

19. KEY WORDS *(Continue on reverse side if necessary and identify by block number)*

Auroral kilometric radiation	Plasma waves
Parametric interactions	Plasma radiation
Nonlinear waves	Coherent wave amplification
Kinetic three-wave interaction	Beams in plasmas

20. ABSTRACT *(Continue on reverse side if necessary and identify by block number)*

We present an extension of the analysis of our previously proposed model for auroral kilometric radiation, in which the full three-wave dynamics is considered. The temporal variation of the electrostatic ion cyclotron density fluctuations and the effect of a finite three-wave coupling coefficient, both effects ignored in our steady state theory, are included here. This yields a set of coupled three-wave kinetic equations, which are solved numerically for the evolution of the auroral kilometric radiation. The numerical results tend to confirm all of the predictions of our steady state theory. The growth rate is found to be determined by the resonant growth rate found in our steady state theory, and stages of the growth are found in which →

(Continues)

DD FORM 1 JAN 73 1473 EDITION OF 1 NOV 65 IS OBSOLETE S/N 0102-LF-014-6601

252950

SECURITY CLASSIFICATION OF THIS PAGE *(When Data Entered)*

20. Abstract (continued)

the radiation grows at twice the resonant growth rate, and sometimes four, eight, etc. times that value. The growth saturates, and this saturation level is found to scale as $\Gamma_b^{4/3}$, where Γ_b is the rate of transfer of energy from the beam to the beat wave, or quasimode. Saturation levels are found which are adequate to produce the observed radiation levels. It is found that for a sufficiently large growth region, the saturation level is relatively independent of the initial level of density fluctuations.

CONTENTS

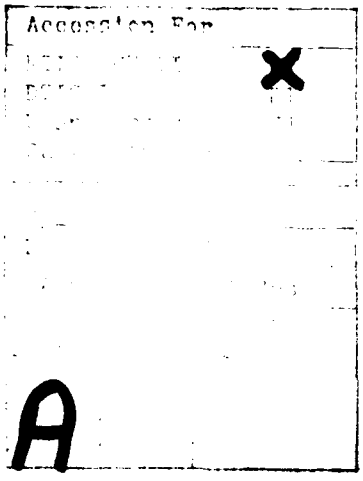

A COHERENT NONLINEAR THEORY OF AURORAL KILOMETRIC RADIATION: II. DYNAMIC INTERACTIONS

I. Introduction

In a recent paper [Grabbe, et al. 1980], a theory of auroral kilometric radiation was proposed, in which electromagnetic noise is amplified by interaction with low frequency coherent quasineutral density fluctuations created by electrostatic ion cyclotron (EIC) waves, in the presence of precipitating auroral electron beams. The result is a three-wave parametric process in which a beat wave is produced that can interact with the beam, much like the theory of Palmadesso, et al [1976]. It was found that when the wave frequency is in the right range, the electromagnetic wave is negative energy in the rotating frame of the beam electron and undergoes a convective instability. The basic requirements for the instability were found to be:

(1) Minimum beam density:

$$\left(\frac{n_b}{n_o}\right) > \frac{k_z(\Delta v)^2}{2\omega_{ce} v_b} \tag{1}$$

where n_b and n_o are the beam and plasma density, respectively, v_b and Δv the beam velocity and thermal spread in velocity space, k_z the wave vector component along the magnetic field, and ω_{ce} the electron cyclotron frequency.

(2) Accessibility to free space ($\omega > \omega_R$ where ω_R is the right hand cutoff):

$$\omega_{pe}^2 < k_z v_b \omega_{ce} \tag{2}$$

Manuscript submitted November 7, 1980.

(3) Frequency range:

$$\omega \lesssim \omega_{ce} + k_z v_b \tag{3}$$

Condition (1) typically requires $n_b \gtrsim 10^{-3} n_{o\,s}$ and condition (2) typically requires local depletion of the plasma density such that $\omega_{pe} \lesssim 0.2\ \omega_{ce}$. The latter is in very good agreement with the observed density depletion [Benson and Calvert, 1979].

Combining conditions (1) - (3) gives the following limits on the frequency and propagation directions of the wave for amplification

$$\omega_{ce} + \frac{\omega_{pe}^2}{\omega_{ce}} < \omega < \omega_{ce} + k_z v_b \tag{4}$$

$$\frac{\omega_{pe}^2}{k v_b \omega_{ce}} < \cos\theta < \frac{2\omega_{ce} v_b n_b}{k (\Delta v)^2 n_o} \tag{5}$$

Eq. (4) gives radiation in a narrow frequency just above the right band cutoff, while Eq. (5) normally limits the propagation to be almost (but not quite) perpendicular to the magnetic field [Grabbe, 1980]. Furthermore, the O-mode has no such unstable frequency range, hence the X-mode is the predicted polarization. All of these predictions are in excellent agreement with observation.

The above conclusions were based on a steady state model, in which amplitude of the density fluctuations was assumed to be approximately constant. This is valid if the energy in the density fluctuations is replenished by the beam or other sources at approximately the same rate as it is being used up. However, the Feynman diagram

for the three-wave process (Fig. 1) reveals that a more dynamical process is taking place. Not only is energy being resonantly transferred from the density fluctuation to the electromagnetic wave in the appropriate frequency band because of the beam, but the energy the beam injects into the beat wave is being transferred back to the density fluctuations and the electromagnetic wave because of a finite three wave coupling coefficient. This coupling coefficient was ignored in the steady state theory, but must be included to understand the full dynamical process.

The purpose of this paper is to study the dynamics of the full three wave process, including temporal variations in the density fluctuations and a finite three-wave coupling coefficient, in order to confirm the predictions of the steady state theory. In Sec. II we introduce a set of coupled nonlinear rate equations for the evolution of each of the three waves in the Feynman diagram, and discuss steady state solutions. Several numerical solutions of these equations are presented and discussed in Sec. III for various typical parameters. The principle conclusions are summarized in Sec. IV.

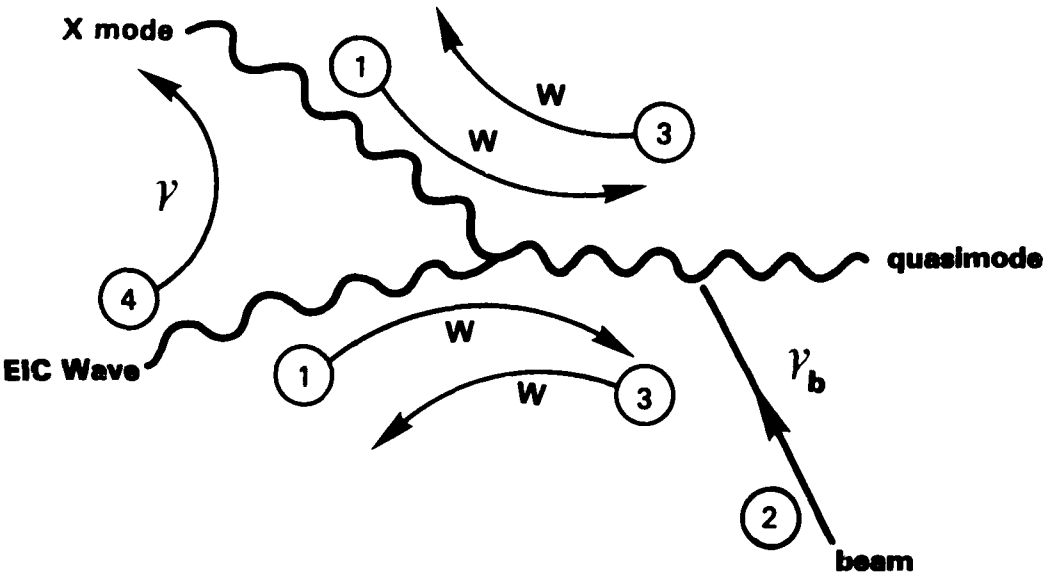

Fig. 1 — Feynman diagram for the three-wave interaction involved in the amplification of radiation to produce auroral kilometric radiation. The processes numbered are (1) induced absorption, (2) beam amplification, (3) induced (and spontaneous) emission, and (4) resonant amplification. The rate coefficient for each process is shown.

II. Dynamical Model

The dynamical processes involved in the amplification process which produces the AKR are summarized in the three-wave Feynman diagram in Fig. 1. These processes are (1) Induced absorption of the X mode by the density fluctuations to create the quasimode or beat wave (2) Beam amplification of the beat wave (3) Spontaneous and induced emission of the X-mode by the beat mode (4) Resonant interaction between the density fluctuations and the X mode in which energy is transferred to the X mode. The conditions for the last process were given in the introduction, and the resulting spatial growth rate was given by Eq. (28) in Grabbe, et al [1980]:

$$\kappa = \left(\frac{\omega}{c}\right)\left[\left(\frac{\alpha_2}{\alpha_1}\right)^2 \frac{\varepsilon^2}{4} - \left(\frac{\sqrt{\alpha_1}}{k_1} - 1\right)^2\right]^{1/2} \tag{6}$$

We want to formulate the rate equations for the aforementioned processes in terms of the (quantum) occupation number density of the waves.

$$N_j = |\vec{E}_j|^2 / 8\pi\omega_j \tag{7}$$

where $\vec{E}$ is the wave electric field. We designate N_o as the number density of the X-mode, N_1 for the density fluctuations, and N_b for the beat wave. We then have the following contributions to the rate equation for each process numbered in Fig. 1:

(1) Induced absorption.

$$\frac{dN_b}{dt} = - W N_o N_1 \tag{8a}$$

$$\frac{dN_1}{dt} = - W N_o N_1 \tag{8b}$$

$$\frac{dN_b}{dt} = 2W N_o N_1 \tag{8c}$$

where W is the three wave coupling coefficient [Tsytovich, 1974]:

$$W = \frac{e^2 \omega_{ei}^3 \omega_{pe}^2 m_i}{8\pi m_e^3 \omega^3 v_{Te}^4 k^2} \tag{9}$$

(2) Beam amplification.

$$\frac{dN_b}{dt} = \Gamma_b N_b \tag{10}$$

where we take the beam driven growth rate of the quasimode Γ_b to be the usual form for a beam plasma instability [Briggs, 1964]:

$$\Gamma_b = 2 \text{ Im } \omega \sim 1.4 \left(\frac{n_b}{n_o}\right)^{1/3} \omega_{pe} \tag{11}$$

(3) Spontaneous and induced emission.

$$\frac{dN_o}{dt} = W N_b (1+N_o+N_1) \tag{12a}$$

$$\frac{dN_1}{dt} = W N_b(1+N_o+N_1) \tag{12b}$$

$$\frac{dN_b}{dt} = -2W N_b(1+N_o+N_1) \tag{12c}$$

The spontaneous emission term (first term on the right hand) is normally negligible, since normally $N_o >> 1$ or $N_1 >> 1$ (N_o and N_1, taken as dimensionless occupation numbers).

(4) Resonant interaction.

$$\frac{dN_o}{dt} = \gamma N_o N_1^{1/2} \tag{13a}$$

$$\frac{dN_1}{dt} = -\gamma N_o N_1^{1/2} \tag{13b}$$

Here the dependence of the resonant growth rate Γ of the X-mode on the density fluctuation N_1 has been explicitly factored out:

$$\Gamma = \gamma N_1^{1/2} \tag{14}$$

Here the temporal growth rate can be expressed in terms of the spatial growth rate by multiplying by the group velocity

$$\Gamma = 2 \kappa c \tag{15}$$

where the factor 2 represents the conversion between electric field growth rate an the quantum density growth rate. Thus from Eq. (6)

$$\gamma \sim \frac{(2\pi)^{\frac{1}{2}} \alpha_2 \omega^{3/2} e}{\alpha_1 \kappa T_e} \tag{16}$$

at its maximum value.

Combining, (1), (2), (3), (4) we find the complete set of equations to be

$$\frac{dN_o}{dt} = W(N_b N_o + N_b N_1 - N_o N_1) + \gamma N_o N_1^{1/2} \tag{17a}$$

$$\frac{dN_1}{dt} = W(N_b N_o + N_b N_1 - N_o N_1) - \gamma N_o N_1^{1/2} \tag{17b}$$

$$\frac{dN_b}{dt} = 2W(N_o N_1 - N_o N_b - N_1 N_b) + \Gamma_b N_b \tag{17c}$$

These are the central equations we want to solve for AKR evolution.

Before obtaining numerical solutions of the equations we want to first examine them for steady state solutions. If we consider the limit of constant density fluctuations $dN_1/dt = 0$, the case analyzed in our steady state theory, we find

$$\frac{dN_o}{dt} = 2\gamma N_o N_1^{1/2} \tag{18}$$

This result shows that the X-mode grows at twice the rate determined in our steady state [Grabbe, et al.,]980]. This result can be understood by noting the two processes which transfer energy to the X mode: (3) transfers energy from the beat wave to the X mode and density fluctuations at equal rates; (4) transfers energy from the density fluctuation to the X-mode. Both processes (3) and (4) must occur at equal rates for the density fluctuation to achieve a steady state. Since the steady state model only considers the contribution of process (4), it only gives one-half of the growth rate.

III. Numerical Results

To obtain typical values for the growth rates and coupling coefficient we use Eqs. (9), (11) and (16). If we take typical source region values $n_b \gtrsim 10^{-3} n_o$, $\omega_{pe} \lesssim 0.2\ \omega_{ce}$, $n_1 \sim 0.3\text{-}0.5\ n_o$, we find the following normalized values when the N_α's are normalized to dimensionless values

$$\Gamma_b \gtrsim 6 \times 10^4\ \text{sec}^{-1} \tag{19a}$$

$$\Gamma = \tilde{\gamma}\, \tilde{N}_1^{1/2} \gtrsim 6 \times 10^4\ \text{sec}^{-1} \tag{19b}$$

$$\tilde{W} \sim 0.05\ \text{sec}^{-1} \tag{19c}$$

Here $\tilde{N}_\alpha = (e^2/m_e^2 c^2 \omega) N_\alpha$, $\tilde{\gamma} = (e/m_e c\sqrt{\omega}\,)$ and $\tilde{W} = (m^2c^2/e^2)W$. These values will be used as a guide for input to the numerical calculations.

The kinetic equations in Eq. (17) were solved for several values of the growth rate and initial conditions, although the initial value of N_1 was always set to the normalized value on 1. A classical Runge-Kutta integration routine was used initially but proved to be too inefficient, so it was replaced by a stiff integration scheme called CHEMEQ [Young, 1980]. A sampling of the results is shown in Figs. 2-4. Included in the graphs is the ratio of the time dependent growth rate $\Gamma^*(t)$ to the resonant growth rate Γ, where

$$\frac{dN_o}{dt} \equiv \Gamma^*(t) N_o \quad . \tag{20}$$

The graphs show that there are two principle stages of growth of the X-mode. In the initial stage the growth rate is just the resonant growth rate $dN_o/dt = \gamma N_o N_1$. The reason for this stage is that not much energy has been transferred into the beat wave, so all of the X-mode energy is coming from the density fluctuations. This stage

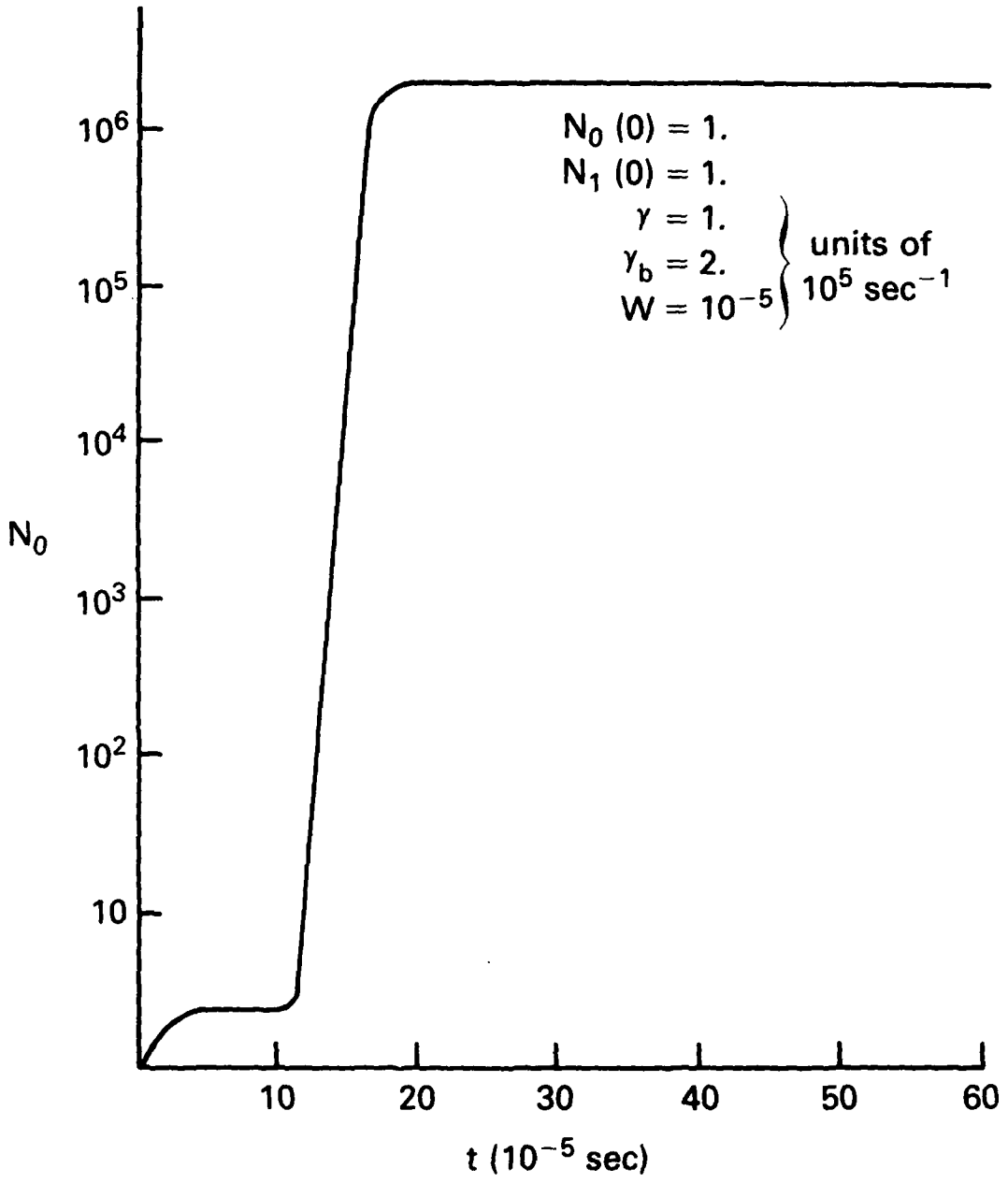

Fig. 2 — Growth and saturation of the X mode radiation for the initial conditions and rate coefficients shown. The values shown are for the normalized form given by Eq. (19). Note that the radiation grows in two principal stages: in the first, the wave grows primarily on energy from the EIC density fluctuations, and temporarily saturates; in the second the wave grows to very large amplitudes because of energy coupled in from the beam via a beat wave then finally saturates.

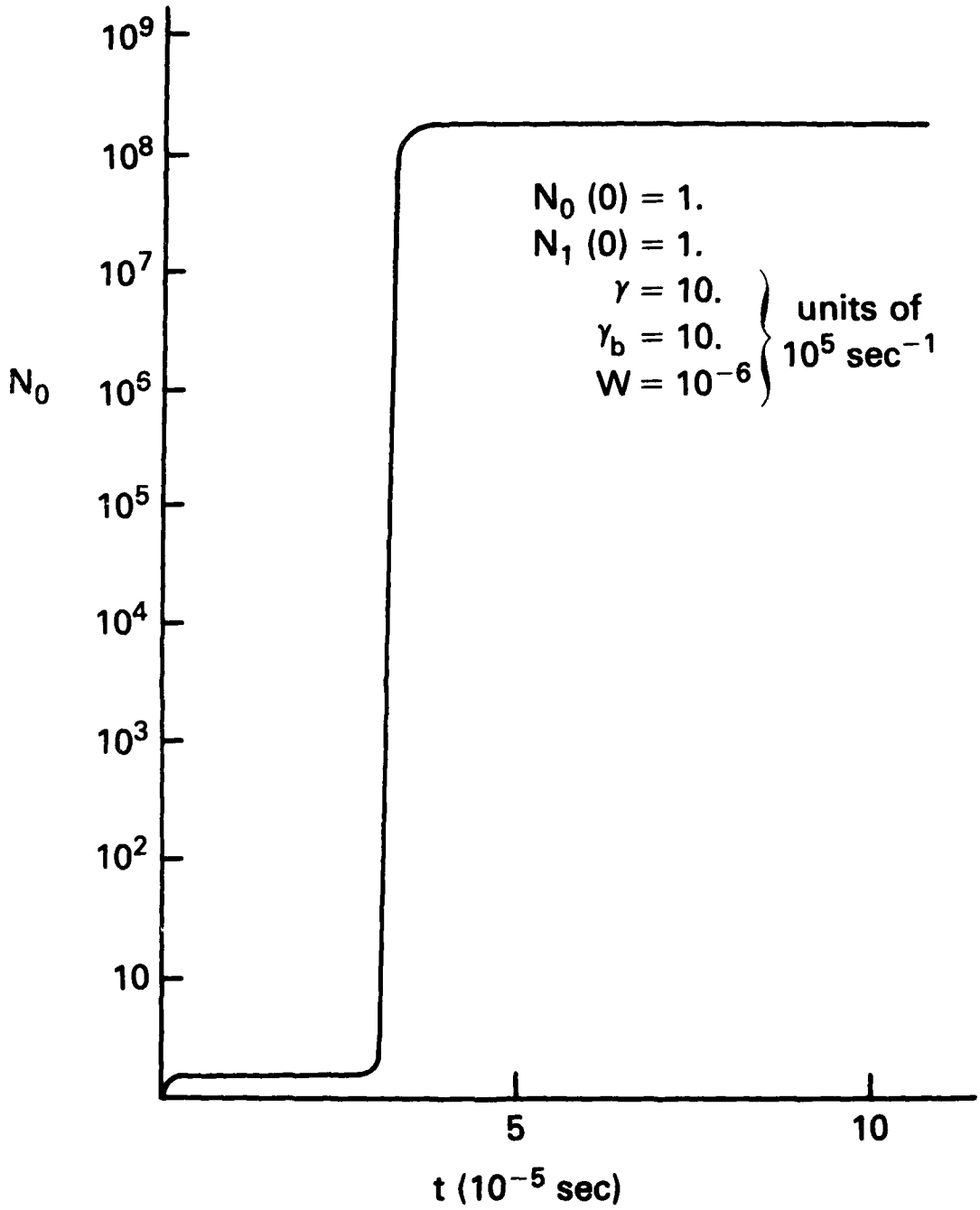

Fig. 3 — Same as Fig. 2 for a slightly different set of rate coefficients.

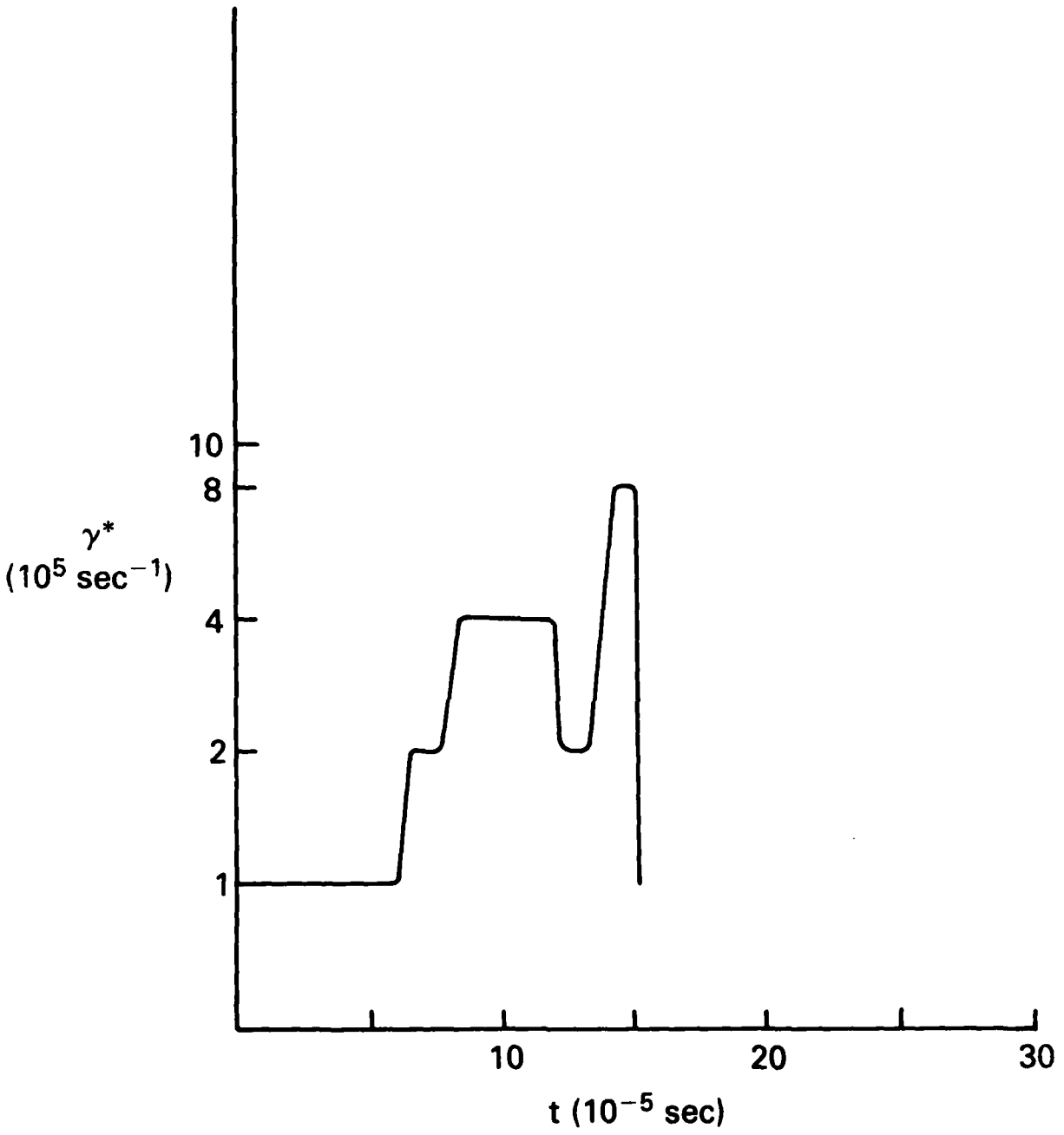

Fig. 4 — Graph of the ratio of the growth rate of the wave as function of time to that found in the steady state theory, for the conditions in Fig. 3. Note that it is normally 2^n, for various non-negative integer values of n.

normally saturates when most of the energy in the density fluctuations is absorbed. The second stage starts when a significant amount of energy has been pumped into the beat wave by the beam, and this energy begins being transferred to the density fluctuations and the X-mode. This second stage grows at $dN_o/dt=2\gamma N_o N_1^{\frac{1}{2}}$, or twice the resonant growth rate. The graphs of $\Gamma^*(t)/\Gamma=\gamma^*(t)/\gamma$ shows there may also exist subsequent stages in which the growth rate occurs at $dN_o/dt=4\gamma N_o N_1^{\frac{1}{2}}$, $dN_o/dt=8\gamma N_o N_1^{\frac{1}{2}}$ etc. Then the process reaches a final level of saturation when almost all of the energy of the density fluctuations and the beat wave has been depleted. The stages of growth confirm that the rate of growth is governed by the resonant growth rate $\Gamma=\gamma N_1^{\frac{1}{2}}$, as predicted by the steady state theory.

A comparison of the saturation amplitude of the X-mode shows that it always is several orders of magnitude above the initial value of the density fluctuations $N_1(t=0)$. This shows that virtually all of the energy comes from the beam, rather than from the initial level of the density fluctuations. Furthermore, when Γ_b is varied on sample runs with all other parameters being held constant, then the saturation amplitude increases as Γ_b is increased; thus, Γ_b determines the total energy the electromagnetic wave can absorb. A statistical analysis of the saturation level $N_{o\ sat}$ from many sample runs reveals the scaling law

$$N_{o\ sat} \sim \Gamma_b^{4/3} \tag{21}$$

From Eq. (11), we have the dependence on the relative beam density

$$N_{o\ sat} \sim \left(\frac{n_b}{n_o}\right)^{4/9} \tag{22}$$

A derivation of this scaling law is given in the Appendix.

A comparison has been made on sample runs for different initial values of N_1, all other parameters held constant. It is found that although the growth rate of the X mode increases linearly with N_1, the saturation amplitude is relatively independent of the initial value of N_1! The significance of this for the growth process in the finite density depleted cavity introduced in the steady state model [Grabbe, et al., 1980] is the following. If the X-mode saturates before propagating out of the growth region in the cavity, then an increase in the initial levels of the density fluctuations does not have a very important effect on level of AKR produced. However, if the X-mode propagates out of the growth region before reaching its saturation level, increasing the initial level of the EIC density fluctuations would bring the AKR closer to its saturation value. Calculation done in the steady state model would suggest the former case occurs more often than the latter.

IV. Summary and Conclusions

We have formulated the dynamics of the three-wave process involved in amplification of the X-mode to produce AKR in terms of a set of coupled rate equations. An analysis of these coupled rate equations has confirmed the conclusions drawn from the steady state theory. It was found that the growth rate was determined by the resonant growth rate found in the steady state. The growth was seen to occur in stages: an initial stage in which the growth rate was just the resonant growth rate, and subsequent stage of growth at 2^n times the resonant growth rate, where n=1,2,3,.... This is followed by a saturation of the wave.

It was found that the AKR could saturate at 10^8-10^{10} times the initial (noise) levels. This is adequate to produce the observed levels of AKR. Almost all of this energy comes from the beam, and the saturation amplitude was seen to scale as $\Gamma_b^{4/3}$, so that the growth rate of the beat wave determines the total energy the electromagnetic wave can absorb. Finally, it was found that for sufficiently large density cavities with growth regions, the saturation level of AKR is relatively independent of the initial level of the EIC density fluctuations.

ACKNOWLEDGMENTS

We gratefully acknowledge support for this research by NASA and the Office of Naval Research.

References

Benson, R. and W. Calvert, Isis I observations at the source of auroral kilometric radiation, Geophys. Res. Lett., 6, 479, 1979.

Briggs, R. J., Electron Stream Interactions in Plasma, M.I.T. Press, Boston, 1964.

Grabbe, C., P. Palmadesso, and K. Papadopoulos, A coherent nonlinear theory of auroral kilometric radiation: I. Steady state theory, J. Geophys. Res., 85, 659, 1980.

Palmadesso, P., T. Coffey, S. Ossakow and K. Papadopoulos, Generation of terrestrial kilometric radiation by beam driven electromagnetic instability, J. Geophys. Res., 81, 1762, 1976 .

Tsytovich, V., Nonlinear Effects in Plasma, Appendix 3, Plenum Press, New York, 1970.

Young, T., CHEMEQ - A subroutine for solving stiff ordinary differential equations, Naval Res. Lab. Memo Rpt. #4091, 1980.

DISTRIBUTION LIST

Director
Naval Research Laboratory
Washington, D.C. 20375
Attn: T. Coffey (25 copies)
J. Brown
S. Ossakow (100 copies)

University of Alaska
Geophysical Institute
Fairbanks, Alaska 99701
Attn: Library

University of Arizona
Dept. of Planetary Sciences
Tucson, Arizona 85721
Attn: J. R. Jokipii

University of California, S. D.
LaJolla, California 92037
(Physics Dept.):
Attn: J. A. Fejer
T. O'Neil
Vu Yuk Kuo
J. Winfrey
Library
J. Malmberg
(Dept. of Applied Sciences):
Attn: H. Booker

University of California
Los Angeles, California 90024
(Physics Dept.):
Attn: J. M. Dawson
B. Fried
J. G. Moralles
Y. Lee
A. Wong
F. Chen
Library
R. Taylor
(Institute of Geophysics and
Planetary Physics):
Attn: Library
C. Kennel
F. Coroniti

Columbia University
New York, New York 10027
Attn: R. Taussig
R. A. Gross

University of California
Berkeley, California 94720
(Space Sciences Laboratory):
Attn: Library
M. Hudson
(Physics Dept.):
Attn: Library
A. Kaufman
C. McKee
(Electrical Engineering Dept.):
Attn: C. K. Birdsall

University of California
Physics Department
Irvine, California 92664
Attn: Library
G. Benford
N. Rostoker
C. Robertson
N. Rynn

California Institute of Technology
Pasadena, California 91109
Attn: R. Gould
L. Davis, Jr.
P. Coleman

University of Chicago
Encrico Fermi Institute
Chicago, Illinois 60637
Attn: E. N. Parker
T. Lerche
Library

University of Colorado
Dept. of Astro-Geophysics
Boulder, Colorado 80302
Attn: M. Goldman
Library

Cornell University
Laboratory for Plasma Physics
Ithaca, New York 14850
Attn: Library
R. Sudan
B. Kusse
H. Fleischmann
C. Wharton
F. Morse
R. Lovelace

Harvard University
Cambridge, Massachusetts 02138
Attn: Harvard College
Observatory (Library)
G. S. Vaina
M. Rosenberg

Harvard University
Center for Astrophysics
60 Garden Street
Cambridge, Massachusetts 02138
Attn: G. B. Field

University of Iowa
Iowa City, Iowa 52240
Attn: C. K. Goertz
G. Knorr
D. Nicholson

University of Houston
Houston, Texas 77004
Attn: Library

University of Michigan
Ann Arbor, Michigan 48104
Attn: E. Fontheim

University of Minnesota
School of Physics
Minneapolis, Minnesota 55455
Attn: Library
J. R. Winckler
P. Kellogg

M.I.T.
Cambridge, Massachusetts 02139
Attn: Library
(Physics Dept.):
Attn: B. Coppi
V. George
G. Bekefi
T. Dupree
R. Davidson
(Elect. Engineering Dept.):
Attn: R. Parker
A. Bers
L. Smullin
(R. L. E.):
Attn: Library
(Space Science):
Attn: Reading Room

Northwestern University
Evanston, Illinois 60201
Attn: J. Denevit

Princeton University
Princeton, New Jersey 08540
Attn: Physics Library
Plasma Physics Lab. Library
M. Rosenbluth
C. Oberman
F. Perkins
T. K. Chu
V. Aranasalan
H. Hendel
R. White
R. Kurlsrud
H. Furth
M. Gottlieb
S. Yoshikawa
P. Rutherford

Rice University
Houston, Texas 77001
Attn: Space Science Library
R. Wolf

University of Rochester
Rochester, New York 14627
Attn: A. Simon

Stanford University
Institute for Plasma Research
Stanford, California 94305
Attn: Library
F. W. Crawford

Stevens Institute of Technology
Hoboken, New Jersey 07030
Attn: B. Rosen
G. Schmidt
M. Seidl

University of Texas
Austin, Texas 78712
Attn: W. Drummond
V. Wong
D. Ross
W. Horton
D. Choi
R. Richardson
G. Leifeste

College of William and Mary
Williamsburg, Virginia 23185
Attn: F. Crownfield

Lawrence Livermore Laboratory
University of California
Livermore, California 94551
Attn: Library
B. Kruer
J. Thomson
J. Nucholls
J. DeGroot
L. Wood
J. Emmett
B. Lasinsky
B. Langdon
R. Briggs
D. Pearlstein

Los Alamos Scientific Laboratory
P. O. Box 1663
Los Alamos, New Mexico 87344
Attn: Library
D. Forslund
J. Kindell
B. Bezzerides
D. Dubois
H. Dreicer
J. Ingraham
R. Boyer
C. Nielson
E. Lindman
L. Thode
B. Godfrey

N.O.A.A.
325 Broadway S.
Boulder, Colorado 80302
Attn: J. Weinstock
Thomas Moore (SEL,R-43)
W. Bernstein
D. Williams

Oak Ridge National Laboratory
P. O. Box V
Oak Ridge, Tennessee 37830
Attn: I. Alexeff
C. Beasley
D. Swain
D. Spoug

Sanda Laboratories
Albuquerque, New Mexico 87115
Attn: A. Toepfer
G. Yeonas
D. VanDevender
J. Freeman
T. Wright

Austin Research Association
600 W. 28th Street
Austin, Texas 78705
Attn: J. R. Thompson
L. Sloan

Bell Laboratories
Murray Hill, New Jersey 07974
Attn: A. Hasegawa

Lockheed Research Laboratory
Palo Alto, California 94304
Attn: M. Walt
J. Cladis

Maxwell Laboratories
9244 Balboa Avenue
San Diego, California 92123
Attn: A. Kolb
A. Mondelli
P. Korn

Physics International Co.
2400 Merced Street
San Leandro, California 94577
Attn: J. Benford
S. Putnam
S. Stallings
T. Young

Science Applications, Inc.
Lab. of Applied Plasma Studies
P. O. Box 2351
LaJolla, California 92037
Attn: L. Linson
J. McBride

Goddard Space Flight Center
Greenbelt, Maryland 20771
Attn: M. Goldstein
T. Northrup

TRW Systems Group
Space Science Dept.
One Space Park
Redondo Beach, California 90278
Attn: R. Fredericks
F. Scarf

National Science Foundation
Atmospheric Research Section (ST)
Washington, D.C. 20550
Attn: D. Peacock

Benson, Robert
Code 620
Goddard Space Flight Center
Greenbelt, Maryland 20771

Cauffman, David
NASA Headquarters
Code ST-5
Washington, D.C. 20546

Chang, Tien
Boston College
20 Demar Road
Lexington, Maryland 02173

Gendrin, Roger
CNET
3 Ave. do la Republique
Issy-les-Moulineaux,
FRANCE 92131

Heyverts, J.
Observatoire
D.A.F. G21GO
Meudon,
FRANCE

Kikuchi, Hiroshi
College of Sci. & Tech.
Nihon University
8, Kanda Surugadai, 1-chome, Chiyoda-ku
Tokyo,
JAPAN 101

deKluiver, H.
FOM-Institute Plasma Physics
P. O. Box 7
3430 AA Nieuwegein,
HOLLAND

Klumpar, David
Center for Space Sciences
P. O. Box 688
University of Texas
Richardson, Texas 75080

Leung, Philip
Dept. of Physics
University of California
405 Hilgard Avenue
Los Angeles, California 90024

Linson, Lewis
Science Applications, Inc.
P. O. Box 2351
LaJolla, California 92037

Lysak, Robert
Space Sciences Lab.
University of California
Berkeley, California 94720

Rodriguez, Paul
Phoenix Corp.
1600 Anderson Road
McLean, Virginia 22102

Schulz, Michael
Aerospace Corp.
A6/2451, P. O. Box 92957
Los Angeles, California 90009

Shawhan, Stanley
Dept. of Physics & Astronomy
University of Iowa
Iowa City, Iowa 52242

Temerin, Michael
Space Science Lab.
University of California
Berkeley, California 94720

Vlahos, Loukas
Dept. of Physics
University of Maryland
College Park, Maryland 20742

Wright, Bradford
Los Alamos Scientific Laboratory
Mail Stop 650
Los Alamos, New Mexico 87545

Wu, Ching Sheng
Inst. of Physical Sci. and Tech.
University of Maryland
College Park, Maryland 20742

Matthews, David
IPST
University of Maryland
College Park, Maryland 20742

Zanetti, Lawrence
Applied Physics Lab.
SIP/Johns Hopkins Road
Laurel, Maryland 20810